

Morphology and optical properties of bare and polydiacetylenes-infiltrated opals

D. Comoretto^{a,*}, F. Marabelli^b, C. Soci^b, M. Galli^b,
E. Pavarini^b, M. Patrini^b, L.C. Andreani^b

^a INFN, INSTM and Dipartimento di Chimica e Chimica Industriale, Università di Genova, Genova, Italy

^b INFN and Dipartimento di Fisica "A. Volta", Università di Pavia, Pavia, Italy

Abstract

Polystyrene artificial opals have been grown by slow gravity sedimentation from aqueous suspension of monodisperse nano-spheres of different diameters. These opals have been infiltrated with diacetylenic monomers, which have been subsequently polymerized. The morphology of the surface has been characterized by atomic force and scanning electron microscopies. In addition, a careful micro-optical characterization of these samples has been performed. The photonic band structure of the opals was derived from variable-angle micro-reflectance measurements and favorably compared with that theoretically calculated.

© 2003 Elsevier Science B.V. All rights reserved.

Keywords: Photonic crystals; Artificial opals; Polydiacetylenes

1. Introduction

Among photonic crystals, artificial opals are widely investigated as three-dimensional (3D) systems. In spite of the larger difficulties in growing 3D photonic crystal instead of the two-dimensional ones, recent improvements in opals quality [1], light guiding properties [2] and infiltration with active materials [3] make them very interesting both from the fundamental and device-oriented points of views. Stimulated by these results, we grew artificial opals and we attempted to infiltrate them with polydiacetylenes, a family of conjugated polymers known for their high and fast nonlinear optical response [4]. The main optical features of the opals used for the infiltration have been previously reported by probing large area silica [5] and polystyrene [6] samples. In the present paper, a new home-made experimental set-up probing areas of about 100 μm diameter has been used to investigate the reflection and diffraction properties of opals. The variable-angle reflectance measurements showed well pronounced features related to the pseudo stop band at the point L of the photonic band structure as well as to its angular dispersion. These data are accounted for by theoretical calculations based on the plane-wave expansion method.

2. Experimental

Polystyrene artificial opals with different sphere diameters (222 and 426 nm, refractive index 1.59) are grown by gravity sedimentation and evaporation of commercial monodisperse sphere suspensions (Duke Scientific). Two different geometrical configurations are employed to grow films and bulk opals. In the first case, two glass or fused silica windows are sandwiched with a spacer and the sphere suspension are inserted from the top allowing the sedimentation of the particles on the walls for several weeks. After full sedimentation and drying, the two glasses are separated leaving the opal films either in one or in the other wall. Bulk opals are obtained by filling with the sphere suspensions a glass tube with a window sealed at the bottom and again by allowing the sedimentation and drying for several weeks. Gentle annealing of the opals is performed at 100 °C for few minutes. The opals have a chalk-like appearance but if observed at near normal incidence, bright green reflections are seen for 222 nm spheres while no colored reflection are visible for the 426 nm ones, except for grazing incidence where a pale red is observed.

The 1,6-di(*N*-carbazolyl)-2,4-hexadiyne (DCHD monomer used for infiltration was synthesized according to the procedure reported in [7]. Infiltration was performed in two ways. The DCHD/methanol solution is cast onto the opal film or dropped between the sandwiched glasses where opal films were grown, thus percolating inside the films. After

* Corresponding author. Tel.: +39-010-3538736;

fax: +39-010-3536199.

E-mail address: comoretto@chimica.unige.it (D. Comoretto).

this process was recursively repeated, the impregnated films were left to spontaneously polymerize in standard laboratory conditions. The spontaneous polymerization process has been roughly monitored by the change in the color of the sample, being the monomer transparent and the polymer (polyDCHD) dark due to its absorption in the visible spectrum.

The opal surface is characterized by atomic force microscopy (AFM) by an Autoprobe CP-Research ThermoMicroscope. Non-contact-mode topography and topography error (defined as the difference between the cantilever height and the set-point position as obtained from the z-feedback loop) signal images are recorded. A Leo Stereoscan 440 by LEO Electron Microscopy Ltd. is used for scanning electron microscopy (SEM).

Variable-angle specular reflectance was measured in the 0.4–4 eV spectral range by means of a Fourier-Transform spectrophotometer Bruker IFS66. The light of a Xe arc-lamp was collimated and then focused to a spot of 100 μm diameter on the sample surface. The sample was placed on an home-made θ – 2θ goniometer, that allows incidence angles to be varied between 5 and 70°, with an angular resolution of 1°.

3. Results and discussion

The complex morphology of the opal film surface has been previously discussed [6]. We summarize here the main results obtained. AFM images have shown three kinds of regions with different spheres packing: a triangular lattice, a square lattice and disordered regions. In the samples used for this study, the density of square packing regions seems to be lower with respect to those previously investigated [6]. Fig. 1 left shows an AFM topography image of the opal film surface grown with 222 nm spheres. A triangular packing of the spheres is observed in addition to several kind of defects like dislocations (right high corner, bottom), sphere vacancies (black holes), isolated spheres on the surface (white spheres in the middle) and stacking faults (left high corner). These

faults could be very detrimental for the optical response of the opals, but the analysis of the surface profile along the white line indicates the presence of a terrace with a small step (about 20 nm) with respect to the level of the other plane (Fig. 1, right panel). Light scattering effects induced by this roughness are not so strong to mask the photonic properties of the opal indicating the quite good quality of our systems. More important, as discussed below, is the relative rotation of the two domains separated by the stacking fault. Sphere vacancies are also observed as dips in the surface profile while the regular sphere disposition is responsible for the wavy profile.

A preliminary attempt to infiltrate the opal films was performed. As previously described two ways were chosen. First, we drop-coated the surface of the opal with a DCHD methanol solution and allowed its spontaneous polymerization. The results of this procedure are shown in Fig. 2 where a SEM image of a 426 nm spheres opals infiltrated with DCHD is reported. The polymer film seems to cover the opal in a quite homogeneous way, but it is difficult to establish the degree of monomer penetration inside the opal interstices. The second procedure consisted in filling the space between the two glasses where the opals were grown with the solution. In this case, poor results were obtained since all the cracks in the opal films become preferential percolation pathways for the solution without filling the sphere interstices. Further studies on the degree of opal infiltration with conjugated polymers and molecules are in progress.

Being the morphological properties of our opal films well understood, we performed a detailed optical analysis of the samples. In our previous papers, we investigated the transmittance and reflectance properties of both polystyrene and silica opals by using large area (about 1 cm^2) light probes of a standard spectrophotometer beam [5,6]. As a matter of fact, the spectra clearly showed a strong feature and, by varying the incidence angle, its dispersion. This fact can be easily understood by means of the photonic band structure calculated for a face-centered-cube (fcc) close packed spheres lattice (Fig. 3, left panel), which predicts a pseudo stop band at the L (1 1 1) point of the Brillouin zone. This point corresponds

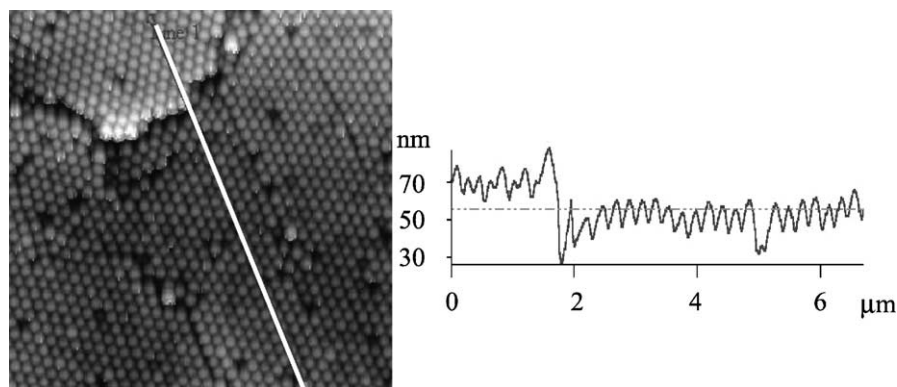


Fig. 1. Left panel: AFM topography image of a 6.7 μm \times 6.7 μm surface of an opal film with 222 nm spheres. The white line indicates the region where the height profile (right panel) is recorded.

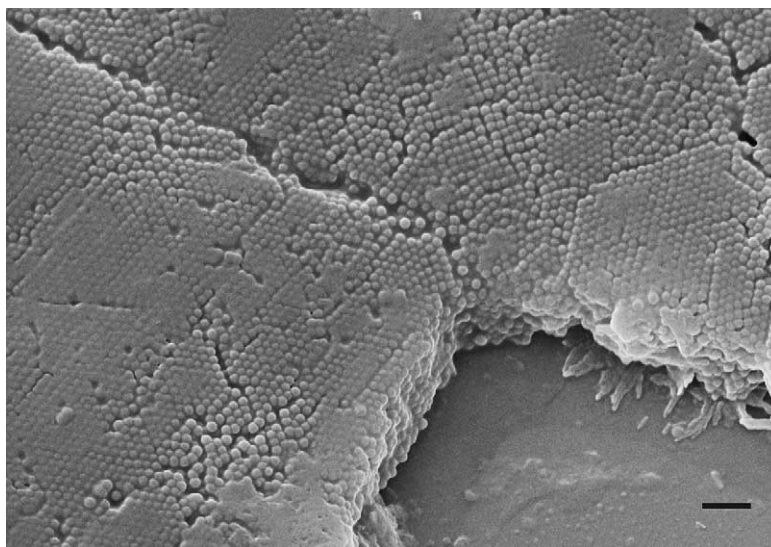


Fig. 2. SEM images of a 426 nm opal infiltrated with polyDCHD. The black bar is 2 μm long.

to a surface with triangular packing of the spheres as experimentally observed in the surface of the samples (Fig. 1). Moreover, by reducing with a diaphragm the dimension of the probing spot to 1 mm^2 , an improvement of the intensity and a reduction of the bandwidth of the photonic spectrum was achieved indicating that the smaller spot allows the se-

lection of more ordered regions of the sample [6]. This observation stimulated further work in the field and allowed to set-up a new experimental facility, which allows to probe areas as small as 100 μm diameter over a broad spectral range. Even though much smaller probing area where recently used to investigate the optical response of opals [8], our set-up has

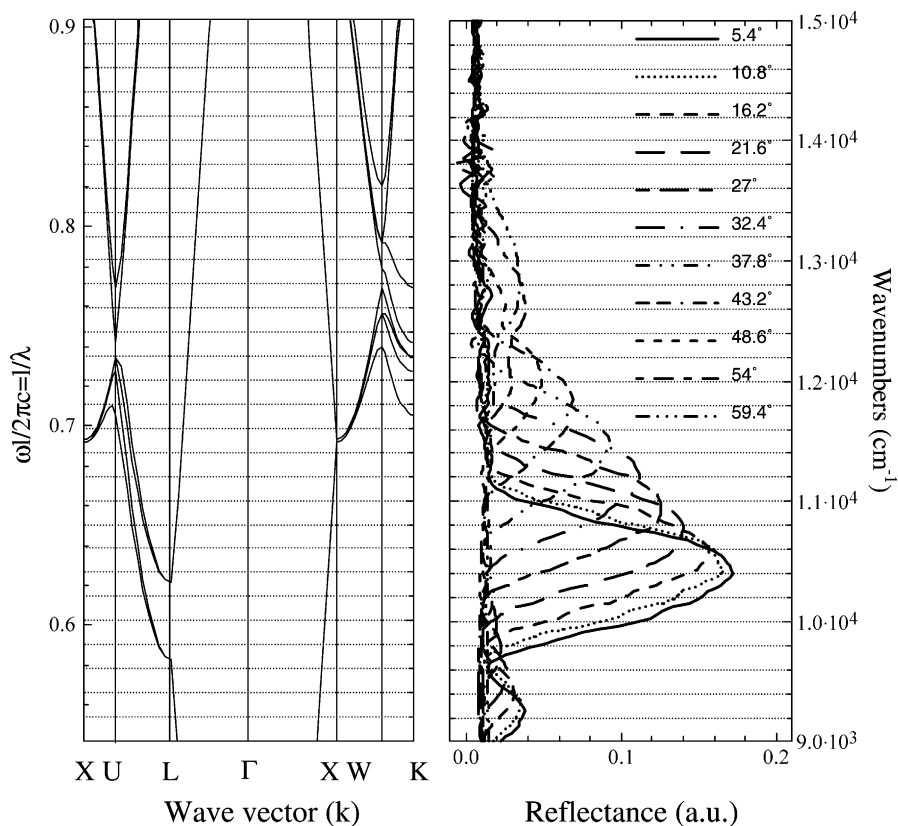


Fig. 3. Left panel: Photonic band structure calculated for 426 nm polystyrene spheres assembled in a close-packed fcc lattice (opal). Right panel: Variable-angle micro-reflectance measurements of a 426 nm polystyrene opal film.

the advantage to cover a broader spectral range combined with a good angular resolution ($\pm 1^\circ$). Fig. 3 right shows the variable-angle reflectance spectra of a 426 nm opal film. The reflectance is referred to that of the glass substrate. Even though the signal is not very high, it can be easily detected and in the near infrared spectral region (not shown here) a progression of interference fringes is observed indicating a good thickness homogeneity of the sample within the spot area. We notice that no variation of the signal is observed upon rotation of the opal around the normal to its surface thus indicating that the light spot probes a number of crystalline domains randomly oriented as observed in the AFM images (see Fig. 1, left panel). This is consistent with the SEM images showing that crystallites with triangular packing are randomly oriented with respect each other and are separated by disordered regions. This texture can be also observed in Fig. 2 for an infiltrated sample.

The main feature in the reflectance spectra of the opal films at near normal incidence (minimum angle 5.4°) is peaked at $10,400\text{ cm}^{-1}$ being due to the pseudo-gap at the point L. This feature shifts toward higher energies and loses its intensity by increasing the incidence angle. In addition, new features are observed at about $12,600\text{ cm}^{-1}$ for incidence angles above 48.6° , which evolves in a complicated way. The comparison of the optical data with the photonic band structure shows several things. The spectral position of the stop-band at near-normal-incidence matches within 400 cm^{-1} with the calculated value (the center of the pseudo-gap at the L point) for a close packed face-centered-cube 426 nm spheres lattice. By considering that the measurements are not truly at normal incidence (5.4°) and that the close packed condition is not matched in all the probed sample volume, we found an excellent agreement between theory and experiment, in particular if we notice that no free parameters are allowed for the calculation. Notice that with large area spots, the agreement was within 0.1 eV ($\sim 800\text{ cm}^{-1}$) [6] again indicating the optical quality of the investigated surface. The full width half maximum of the stop band is about 800 cm^{-1} , i.e. very similar to what theoretically predicted for an ideal opal (roughly estimated as the gap amplitude at L, $\sim 600\text{ cm}^{-1}$). Being the width related to the presence of defects and to their distribution [8,9], we deduce that they do not affect too much the optical response thus allowing for a deeper investigations. The dispersion of the pseudo-stop band with the incidence angle (photon momentum parallel to the surface) is very well accounted for by the calculations. Above $12,000\text{ cm}^{-1}$, the spectra become very complex and it is difficult to make a careful comparison with the theory. However, preliminary

calculations of the density of photonic states indicate the presence of structures related to the dispersion surface (the sections at constant energy of the band structure). They correspond to diffracted beams in the opal which appear as Rayleigh-type anomalies in the reflectance spectra. A more detailed work on the assignment of the high-energy spectral region responsible for these effects is currently in progress with higher quality bulk opals [10].

In conclusion, we showed that the opal films we grew are quite ordered and allow for the comprehension of interesting physical aspects of the light–matter interaction in photonic crystals. The infiltration of these opals with diacetylenes and their polymers still need further effort to produce high quality samples.

Acknowledgements

We acknowledge support from the Ministry of the University and Scientific and Technological Research. This work is also partially supported by the Network Organic Semiconductors of the Section E of the National Institute for the Physics of the Matter. The technical help of Marco Moscardini with the AFM measurements is gratefully acknowledged. We are also indebted with M. Michetti and C. Uliana for the SEM images. D.C. would like to thank Prof. G. Dellepiane for her support to this work.

References

- [1] Y.A. Vlasov, X.-Z. Bo, J.C. Sturm, D.J. Norris, *Nature* 414 (2001) 289.
- [2] W. Lee, S.A. Pruzinsky, P.V. Braun, *Adv. Mater.* 14 (2002) 271.
- [3] M.N. Shkunov, Z.V. Vardeny, M. de Long, R.C. Polson, A.A. Zakhidov, R.H. Baughman, *Adv. Funct. Mater.* 12 (2002) 21; N. Eradat, A.Y. Sivachenko, M.E. Raikh, Z.V. Vardeny, A.A. Zakhidov, R.H. Bauman, *Appl. Phys. Lett.* 80 (2002) 3491; M. Deutsch, Y.A. Vlasov, D.J. Norris, *Adv. Mater.* 12 (2000) 1176.
- [4] D. Grando, G. Banfi, D. Comoretto, G. Dellepiane, *Chem. Phys. Lett.* 363 (2002) 492, and references cited therein.
- [5] D. Comoretto, D. Cavallo, G. Dellepiane, R. Grassi, F. Marabelli, L.C. Andreani, C.J. Brabec, A. Andreev, A.A. Zakhidov, *Mater. Res. Soc. Symp. Proc.* 708 (2002) BB10.19.1.
- [6] D. Comoretto, R. Grassi, F. Marabelli, L.C. Andreani, *Mater. Sci. Eng. C* 23 (2003) 61.
- [7] R.H. Baughman, K.C. Yee, *J. Polym. Macromol. Rev.* 13 (1978) 219.
- [8] J.F. Galisteo Lopez, W.L. Vos, *Phys. Rev. B* 66 (2002) 036616-1.
- [9] Y.A. Vlasov, V.N. Astratov, A.V. Baryshev, A.A. Kaplyanskiy, O.Z. Karimov, M.F. Limonov, *Phys. Rev. B* 61 (2000) 5784.
- [10] D. Comoretto, L.C. Andreani, et al., in preparation.